Conformational Geometries and Conformation-Dependent Photophysics of Jet-Cooled 1,3-Diphenylpropane

Allan L. L. East, Pedro Cid-Aguero, Haisheng Liu, Richard H. Judge,[†] and Edward C. Lim*[,‡]

Department of Chemistry, The University of Akron, Akron, Ohio 44325-3601

Received: October 12, 1999; In Final Form: December 8, 1999

Rotationally resolved laser-induced fluorescence excitation spectra of the $S_1 \leftarrow S_0$ transitions have been recorded for various conformers of 1,3-diphenylpropane (DPP) in supersonic free expansion. Ab initio simulation of the rotational band contours, based on the S_0 rotational constants from 6-31G(d) MP2 and transition moments from 6-31G(d) CI singles calculations, provides definitive assignments of the four major spectral features to particular torsional isomers. These assignments provide rational explanations for the conformation-dependent excimer formation in jet-cooled DPP.

Introduction

In the very cold environment of a free jet expansion, diarylalkanes stabilize in a number of different conformations, and the structure−property relationship pertaining to elementary photoprocesses can be probed by means of laser-induced fluorescence (LIF) and resonant two-photon ionization (R2PI). During the past few years, we have been studying the manner in which the conformation controls intramolecular excimer formation and photoionization in these species, by comparing the LIF and one-color R2PI spectra of different conformational isomers under identical experimental conditions.

The earlier results on 1,3-diphenylpropane (DPP) have shown that while one conformer, denoted O, exhibits highly efficient excimer formation as well as R2PI, when excited through its low-lying vibronic bands of the $S_1 \leftarrow S_0$ electronic transition, others (labeled A, B, C, and D in the order of increasing transition frequency) do not form excimers or ionize efficiently under the same excitation conditions.[1] The conformer displaying the highly efficient photoprocesses has been identified as the folded g^+g^- rotational isomer, which has two phenyl rings in face-to-face arrangement, Chart 1. Under higher energy excitations, the excimer formation begins to occur from the "extended" conformers as well, but their efficiencies remain conformation-dependent for one-quantum excitation energy up to approximately 1500 cm^{-1} above the electronic origin of S_1.[2] More specifically, the conformer(s) displaying features B and D exhibit much greater efficiency for excimer formation than those displaying features A and C. Although the conformation dependence of the excimer formation[2] allows possible assignments of the spectral bands in terms of the torsional isomers expected for the molecule, i.e., tt, tg^+ (=tg^-, g^+t, g^-t), g^+g^+ (=g^-g^-), and g^+g^- (=g−g+),[3] definitive identification of the conformational geometry requires the determination of the rotational constants for each species.

In this paper, we show that ab initio simulations of the rotational band contours, with no fitting whatsoever, easily provide the assignment of the four origin bands (A, B, C, and D) to three extended conformers of DPP. The structural characterization of the major conformers provides rational explanations for the occurrence of the conformation dependence of excimer formation in DPP.

CHART 1

Methods

Spectroscopy. The rotational fine structure of the high-resolution LIF excitation spectrum was recorded for jet-cooled DPP using a pulse-amplified CW ring dye laser.[4] The ring laser (Coherent 699-29), operating with pyromethene 55% dye (Exciton), was pumped with an argon ion laser (Coherent Innova 200-15). The output of the CW ring laser was seeded in the pulse amplifier (Lambda Physik FL2003), which was in turn pumped by a XeCl excimer laser (Lambda Physik Compex 102). The amplified single-mode laser was frequency-doubled into the near-ultraviolet by a KDP crystal. The ultraviolet laser produces approximately 2 mJ pulse at a repetition rate of 10 Hz, with line width, which is approximately 90 MHz. Absolute calibration of the spectra was performed by simultaneously recording the iodine spectrum using the fundamental of the ring dye laser. A slit aperture oriented parallel to the jet direction was mounted in front of PMT (Hamamatsu 1527P) to reduce the Doppler width. The pulsed, and skimmed, supersonic molecular beam was produced by passing helium (ca. 40 psi) through the heated sample reservoir (70°−90°) and expanding the gas mixture into vacuum through a 0.8 mm pulsed pinhole nozzle (General Value). The fluorescence was collected by the PMT after passing an optical filter (Hoya Optics UV-30).

Computer Simulations of Rotational Band Contour. The ab initio computer simulations proceeded in three stages: geometry optimization, transition moment calculation, and spectrum production. No fitting was performed, except for a rough fitting of the temperature and bandwidth.

In the first stage, geometrical structures for the three extended torsional isomers (tt, tg, and gg) of DPP were optimized using the MP2 level of theory[5] with the 6-31G(d) basis set.[6] We

[†] Permanent address: Department of Chemistry, University of Wisconsin−Parkside, Kenosha, WI 53141-2000.

[‡] Holder of the Goodyear Chair in Chemistry at The University of Akron. E-mail, elim@uakron.edu; FAX, (330) 972-6407.

10.1021/jp993647i CCC: $19.00
Published on Web 01/21/2000

TABLE 1: Ground-State Rotational Constants (cm^{-1}), MP2/6-31G(d)

conformer	A	B	C
tt	0.0515	0.0071	0.0070
gg	0.0410	0.0122	0.0103
tg	0.0477	0.0087	0.0082

initially used semiempirical methods, but we favored MP2 because (i) the semiempirical methods did not produce a stable g^+g^- conformer and (ii) they disagreed with MP2 on the preferred phenyl rotation angles (which can significantly affect transition dipole moment directions). As is default with GAUSSIAN94,[6] this basis set used Cartesian d functions throughout and frozen core orbitals in the correlation step. The symmetries of the resulting three minima were C_{2v} (tt), C_1 (tg), and C_2 (gg), and their energies spanned only a 2 kcal/mol energy range: 0 (gg), 1.1 (tg), and 1.9 (tt). These energy differences are within the accuracy expected of this level of theory, and we will assume that these conformers are essentially isoenergetic. From these geometries, rotational constants were computed and appear in Table 1.

In the second stage, transition dipole moments (TMs) were computed for the two phenyl S_1-S_0 excitations for each of the three rotamers, and results appear in Table 2. This we performed using configuration interaction with only single excitations (CIS)[7] with the 6-31G(d) basis set, because this theory combination has been shown to reproduce the peculiar TMs of alkylbenzenes.[8] We initially tried the semiempirical INDO 1/S method[9] and CIS with smaller basis sets but got inferior results. The TM calculations were run after the optimized Cartesian coordinates were rotated to the principal axis frame, so that the resultant TMs were expressed as components along the *a*, *b*, and *c* principal axes. Only one of the six computed transitions is forbidden by symmetry. Owing to notoriously poor CIS energy predictions,[10] the actual relative and absolute band positions did not correspond well to observed ones; however, the TMs were all that were required of CIS for the rotational contour simulations. Note in Table 2 that net band intensities are computed by multiplying the line strength by the number of minima of each conformation type; this resulted in the prediction of four prominent peaks, which are then candidates for the A, B, C, and D observed peaks.

In the third stage, the rotational lines and intensities are computed and the spectrum is produced. This was done with an asymmetric rotor program[11] modified by us for Gaussian line shapes. This program used for input the following parameters: rotational constants of upper and lower states, the TM vector, temperature, peak full-width-at-half-maximum, and various cutoffs for the spectrum range and size of rotational basis set. We used the S_0 MP2 geometries for the rotational constants of both upper and lower states, and the CIS TM vectors. We found that $T = 0.6$ K and peak width $= 0.02$ cm^{-1} reproduced the experimental spectra well.

All three stages were also performed for the fourth torsional isomer, g^+g^-. Its predicted rotational constants are (*A*, *B*, *C*) = (0.0265, 0.0225, 0.0156). Unfortunately, its relative energy is more sensitive to level of theory (owing to the close interaction of the phenyl rings), making it difficult to predict a Boltzmann correction for its transition intensities. In addition, the simulated rotational fine structure for its allowed transition did not match any of the observed spectra, thus eliminating it from further consideration.

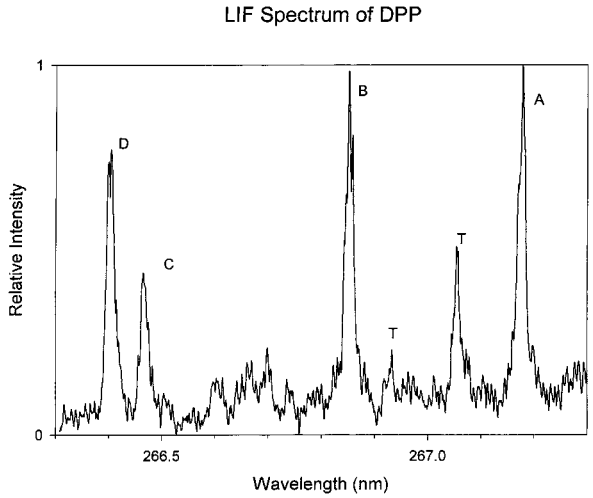

Figure 1. A low-resolution (0.3 cm^{-1}) LIF excitation spectrum of 1,3-diphenylpropane in the region of the $S_1 \leftarrow S_0$ electronic band origins. The peaks are labeled A, B, C, and D in the order of increasing transition frequency. Features labeled T have been assigned to progressions in a torsional mode of conformer A (ref 2).

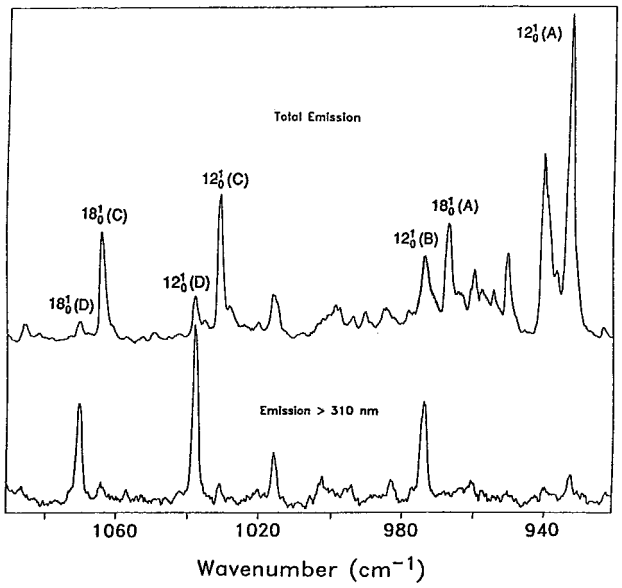

Figure 2. $S_1 \leftarrow S_0$ fluorescence excitation spectra of the total fluorescence (upper trace) and excimer fluorescence (lower trace) in the region of the $S_1 \leftarrow S_0$ 12_0^1 and 18_0^1 transitions. The frequency displacement is with respect to the 0_0^0 band of conformer A at 37 421 cm^{-1} (ref 2).

TABLE 2: Transition Energies, Moments, Intensities, and Assignments, CIS/6-31G(d)

conformer	no. of minima	energy (cm^{-1})	TM vector (au) (*a*, *b*, *c*)	line strength	intensity	assignment
tt	1	49 977	(0.000, 0.173, 0.000)	0.0046	0.0046	C
		49 991	(0.000, 0.000, 0.000)	0.0000	0.0000	
gg	2	49 720	(0.242, 0.000, 0.111)	0.0107	0.0214	A
		49 919	(0.000, 0.050, 0.000)	0.0004	0.0008	
tg	4	49 888	(0.075, 0.074, 0.101)	0.0032	0.0128	D (or B)
		49 991	(0.048, 0.117, 0.028)	0.0026	0.0104	B (or D)

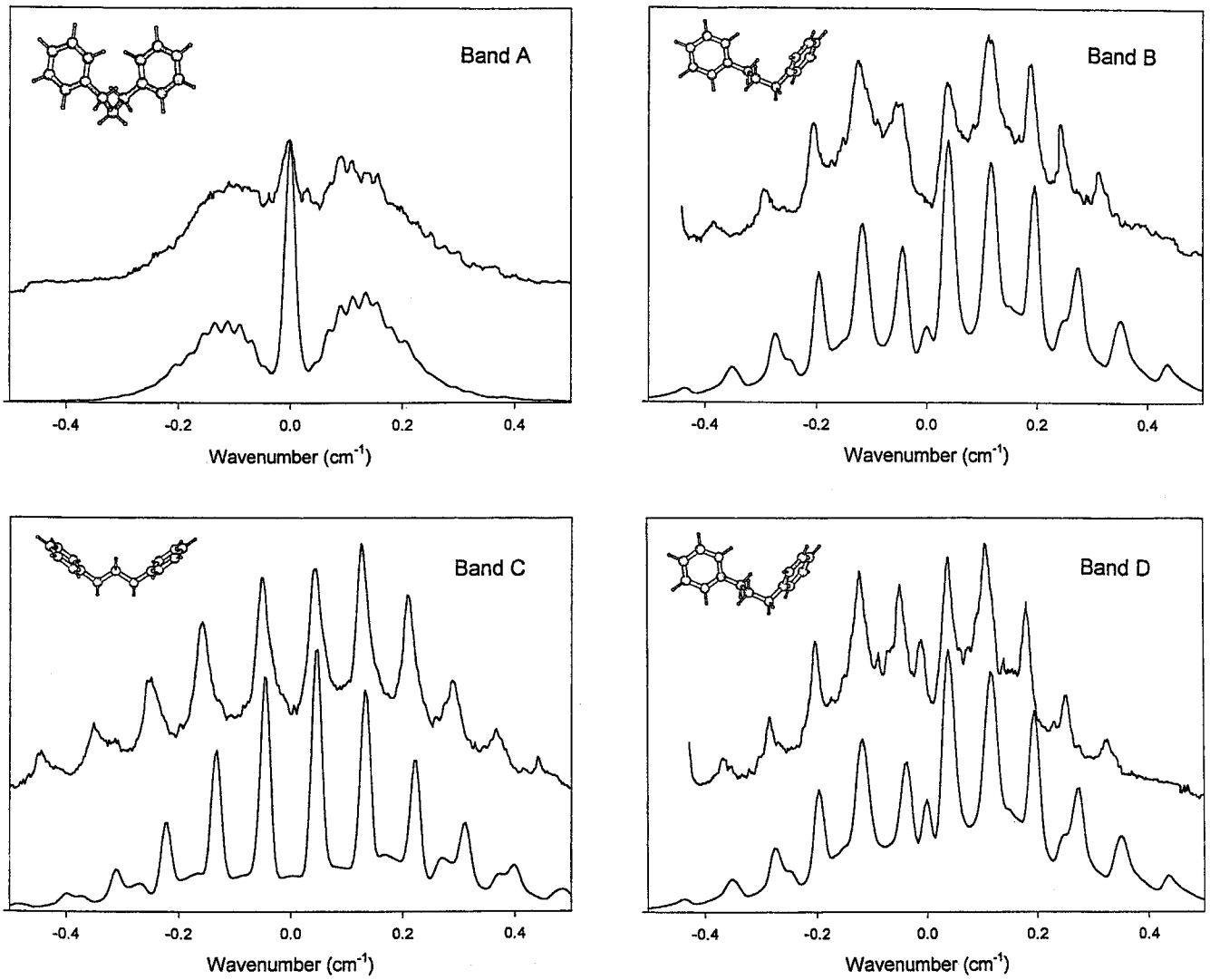

Figure 3. Rotational fine structures of the four $S_1 \leftarrow S_0$ electronic origin bands. In each panel the upper and lower traces represent the experimental and simulated rotational band contours, respectively, and the inset represents the optimized MP2/6-31G(d) geometry for which the simulation is made. The frequency offset is with respect to the band origin, labeled 0.0.

Results and Discussion

Low-Resolution Spectra and Conformation-Dependent Excited-State Dynamics. Figure 1 shows low-resolution LIF excitation spectra of DPP in the region of $S_1 \leftarrow S_0$ 0_0^0 transition. Only four major features, attributable to conformational isomers, appear under normal expansion conditions. Following the earlier work,[2] these peaks are labeled A, B, C, and D in the order of increasing $S_1 \leftarrow S_0$ transition frequency. The band ordering based on the transition frequency, i.e., A < B < C < D, remains the same for the higher vibronic bands.[2]

As previously reported,[2] the formation of an intramolecular excimer in DPP is strongly conformation-dependent. Figure 2 compares the LIF excitation spectra of total fluorescence (dominated by fluorescence from the locally excited state) and excimer fluorescence for the 12_0^1 and 18_0^1 transitions. Figure 2 reveals that the efficiency of the excimer formation varies substantially among the conformers. More specifically, conformers B and D undergo excimer formation efficiently, whereas conformers A and C show little, if any, tendency to form excimers. Similarly, the one-color R2PI of conformer D is significantly greater than that of conformer C with nearly identical transition frequency.[12] The conformation-dependent excimer formation and R2PI erode for excess energies greater than about 1500 cm^{-1}, consistent with the onset of very efficient intramolecular vibrational redistribution (IVR) and resultant thermalization between various conformers.[2]

Structural Assignments of the Major Spectral Features. The rotational fine structures of the four major $S_1 \leftarrow S_0$ electronic origin bands (A, B, C, and D in the order of increasing $S_1 \leftarrow S_0$ transition frequency) are given in Figure 3. In each panel, the upper and lower traces represent the experimental and simulated rotational band contours, respectively, and the inset presents the conformation for which the simulation is made. Note the very good agreement between the theoretical and experimental spectra, considering that no fitting of theory to experiment has been performed (other than rough fitting of temperature and bandwidth). We in fact initially tried fitting model spectra to the observed ones, but obtained multiple solutions and hence ambiguous results. The observed reduction of peak spacings to the blue is not reproduced in the simulations because of our use of equal rotational constants for the upper and lower states. Comparison of the experimental and computed band contours of the 0_0^0 bands allows structural characterization of each conformer in a straightforward manner.

Band A. The previous assignment[2] of band A to the tt rotamer is not supported by the rotationally resolved LIF excitation

spectrum. The correct assignment is the gg rotamer; the simulated band contour for the allowed transition of gg, an *ac*-hybrid band, closely mimics the experimental contour. The electronic transition moment (TM) calculation demonstrates that the predominant *a*-type nature of the rotational band contour has its origin in the vector sum of the two phenyl $S_1 \leftarrow S_0$ TMs, which themselves display the conformationally induced rotation known from studies on *n*-alkylbenzenes.[8] The TM rotation is about 30° with respect to the in-plane short axis of the benzene ring. The assignments[2] of the features labeled T in the LIF excitation spectrum (Figure 1) to progressions in a torsional mode from band A are supported by the near identity of their rotational fine structure to that of band A. The appearance of the torsional progression is an indication that the precise conformation of gg is significantly different in the excited electronic state relative to the ground state along the phenyl torsional coordinate.

Band C. The experimental rotational band contour of band C has the appearance of a perpendicular band of a symmetric top. This is matched by the simulation of the allowed transition of the fully extended tt conformer, whose predicted rotational constants are those of an accidental symmetric top. The most surprising aspect of this assignment is that the CIS calculation places this allowed calculation to the red of the forbidden one, whereas simple "π-electron only" theories place it to the blue.

Bands B and D. On the basis of the observation that the species undergo efficient excimer formation at relatively low excitation energies, bands B and D were initially assigned to the folded g^+g^- and extended tg rotamers, respectively.[2] Subsequent discovery of the O-band and its assignment to g^+g^- suggested that band B is also due to an extended rotational isomer.[1] These two bands are in fact due to the two localized phenyl-group excitations of the tg conformer, from which the folded g^+g^- rotamer can be produced by one rotation about the C_1-C_2 or C_2-C_3 bond (vide infra). These assignments are finalized from our rotational contour work, as demonstrated in Figure 3.

The contours of bands B and D are nearly identical and leave open the question of which band corresponds to which of the phenyl rings in tg. The only striking difference is in the intensity of the central peak, due to the *a*-axis contribution of the transition moment. Our rotational contour simulations suggest that band D, having more *a*-type character, arises from the $\pi^* \leftarrow \pi$ excitation of the *gauche*-phenyl group (the first tg transition listed in Table 2). However, small variances in the predicted C_1-symmetry geometry can alter the degree of a-type character in these hybrid bands, and since band D appears quite near the tt-conformer C-band, it could be due to the *trans*-phenyl group excitation instead.

Remarkably, the integrated experimental intensity ratios of bands A:B(D):C are in close agreement with the predicted intensity ratios in Table 2.

Conformation Dependence of Excimer Formation. The structural characterization of the four spectral features allows rational explanation for the observation[2] that while the conformer(s) of B and D form intramolecular singlet excimer at excess energies about 900 cm^{-1} above their S_1 origin, the conformers of A and C do not exhibit excimer formation until the excess energy reaches about 1500 cm^{-1}. The inefficiency of A and C relative to B and D can best be rationalized using the conformational energy surface for the two internal C−C bonds in *n*-pentane,[3] given in Figure 4. It should be noted that whereas the transformation of tt (C) and gg (A) rotamers to the folded g^+g^- rotamer (precursor for the excimer formation) requires

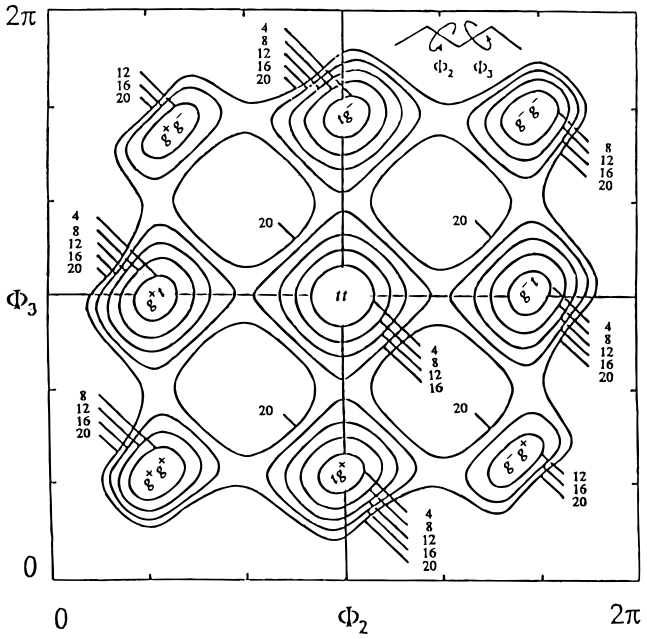

Figure 4. 4. Conformational energy surface for the two internal C−C bonds in *n*-pentane (from ref 3 with permission).

two rotations about C_1-C_2 and C_2-C_3 bonds, only one rotation about C_1-C_2 or C_2-C_3 is required for the conversion of tg (B and D) to g^+g^-. More to the point, the tg rotational isomer is the intermediate state of transition from tt (A) or gg (C) to g^+g^-. It is therefore expected that the excimer formation from photoexcited A and C isomers would be more difficult than that from photoexcited B and D conformers. At sufficiently large excess energies, where efficient intramolecular vibrational redistribution (IVR) and thermal equilibration are expected to occur, the conformation dependence of excimer formation should disappear. The results of the earlier study[2] have indeed shown that the loss of the conformation-dependent excimer formation occurs at excess energies greater than about 1500 cm^{-1}. Interestingly, this excess energy corresponds to the threshold energy at which conformers A and C begin to exhibit excimer formation.

In summary, the structural assignments of the major spectral features of DPP presented herein provide good accounts of the conformation-dependent excimer formation and one-color R2PI that have been observed for the compound. Studies are presently underway to determine ionization potentials (vertical and adiabatic) of individual conformers by two-color threshold photoionization spectroscopy and to probe the energetics and conformational structures of neutral and cationic states of DPP by high-level ab initio quantum chemistry calculations.

Acknowledgment. This work was supported by the Division of Chemical Sciences, Office of the Basic Energy Sciences of the United States Department of Energy.

References and Notes

(1) Cid-Aguero, P.; Liu, H.; Lim, E. C. *Chem. Phys. Lett*. **1997**, *280*, 489.

(2) Chakraborty, T.; Lim, E. C. *J. Phys. Chem*. **1995**, *99*, 17505.

(3) Mattice, W. L.; Suter, V. W. *Conformation Theory of Large Molecules*; John Wiley & Sons: New York, 1994.

(4) Wang, P.-N.; Liu, H.; Lim, E. C. *J. Chem. Phys*. **1996**, *105*, 5697.

(5) Moller, C.; Plesset, M. S. *Phys. Rev*. **1934**, *46*, 618.

(6) Frisch, M. J.; Trucks, G. W.; Schlegel, H. B.; Scuseria, G. E.; Robb, M. A.; Cheeseman, J. R.; Zakrzewski, V. G.; Montgomery J. A.; Stratmann, R. E.; Burant, J. C.; Dapprich, S.; Millam, J. M.; Daniels, A. D.; Kudin, K. N.; Strain, M. C.; Farkas, O.; Tomasi, J.; Barone, V.; Cossi, M.; Cammi,

R.; Mennucci, B.; Pomelli, C.; Adamo, C.; Clifford, S.; Ochterski, J.; Petersson, G. A.; Ayala, P. Y.; Cui, Q.; Morokuma, K.; Malick, D. K.; Rabuck, A. D.; Raghavachari, K.; Foresman, J. B.; Cioslowski, J.; Ortiz, J. V.; Stefanov, B. B.; Liu, G.; Liashenko, A.; Piskorz, P.; Komaromi, I.; Gomperts, R.; Martin, R. L.; Fox, D. J.; Keith, T.; Al-Laham, M. A.; Peng, C. Y.; Nanayakkara, A.; Gonzalez, C.; Challacombe, M.; Gill, P. M. W.; Johnson, B. G.; Pople, J. A. *Gaussian 98*; Gaussian, Inc.: Pittsburgh, PA, 1998.

(7) Foresman, J. B.; Head-Gordon, M.; Pople, J. A.; Frisch, M. J. *J. Phys. Chem.* **1992**, *96*, 135.

(8) Dickinson, J. A.; Joireman, P. W.; Kroemer, R. T.; Robertson, E. G.; Simons, J. P. *J. Chem. Soc., Faraday Trans.* **1997**, *93*, 1467.

(9) Ridley, J.; Zerner, M. *Theor. Chem. Acta* **1973**, *32*, 111; **1976**, *42*, 223.

(10) (a) Foreman, J. B.; Head-Gordon, M.; Pople, J. A.; Frisch, M. J. *J. Phys. Chem.* **1992**, *96*, 135. (b) Roos, B. O.; Andersson, K.; Fulscher, M. P. *Chem. Phys. Lett.* **1992**, *192*, 5.

(11) McKellar, A. R. W.; Watson, J. K. G.; Howard, B. *J. Mol. Phys.* **1995**, *86*, 273.

(12) Cid-Aguero, P.; Lim, E. C. Unpublished results.